Visual Station Keeping and Target Tracking with a Hovering Underwater Vehicle

Conference Paper · September 2014

CITATIONS
0

READS
16

2 authors:

Marc Hildebrandt
Deutsches Forschungszentrum für Künstliche I…
22 PUBLICATIONS **139** CITATIONS
SEE PROFILE

Leif Christensen
Deutsches Forschungszentrum für Künstliche I…
16 PUBLICATIONS **84** CITATIONS
SEE PROFILE

Visual Station Keeping and Target Tracking with a Hovering Underwater Vehicle

Marc Hildebrandt and Leif Christensen
Underwater Robotics Department
DFKI RIC Bremen
Germany, 28359 Bremen
Email: marc.hildebrandt@dfki.de

***Abstract*—Station keeping and target tracking are two valuable features for underwater inspection, but are key requirements in most underwater intervention tasks. In order to precisely manipulate objects, the relative position between vehicle and object should remain constant. Landing or attaching to the structure with an auxiliary manipulator is not always feasible. The resulting tasks of station keeping and target tracking can be divided into two parts: 1) sensing and 2) control.The sensing part deals with estimating the transformation matrix from the vehicle's body frame to either a reference point (station keeping) or an object (target tracking). The control part then uses this information to correct the vehicle position and orientation. While a number of sensor systems can be used to aquire data on relative vehicle motion, this work uses cameras as sensors.**

A. Introduction and Technology Background

In the past years, there has been a trend in the oil and gas industry to extend their operation to deeper regions in the sea. Also an increasing effort in seabed-mining operations of mineral resources and the construction of huge offshore wind parks could be observed. With more and more artificial structures being build onto the sea-floor in ever increasing depth, the need not only for robotic inspection but also for maintenance during operation and removal / renaturation of those infrastructure at the end of their life cycle increases. A frequent approach in the past for close-up inspections of unmanned underwater vehicles, where the vehicle is exposed to external forces coming from currents or an attached umbilical, was to attach the vehicle physically to the object to be inspected. Since this method needs an extra device (e.g. second manipulator) for this method, it is mainly used in the offshore industry, where heavy work-class ROVs equipped with such manipulators are in operation. This approach is not feasible for a large group of vehicles not equipped with a second arm (smaller ROVs, hybrid AUVs or AUVs, etc.), or for situations, in which attaching to the structure could harm or even destroy it (for example because of sensible coatings, in the case of natural structures like reefs, maritime life, etc.).

One approach to tackle the station keeping or (in the dynamic case) target following task is the use of computer vision techniques. Imaging sensors like cameras are widely used in robot perception, both for reactive behaviors [1] and localization [2]. Several algorithms for visual station keeping using monocular or stereo setups and also target tracking in the underwater domain have been proposed [3]–[6], some implemented on vehicles especially designed for the task [7]–[9].

Most of these approaches in the underwater domain face the problem of a lacking reference measurement to evaluate performance and robustness. This work adresses, apart from the developed algorithm itself, specifically the evaluation issue by introducing and applying performance metrices.

I. Algorithms

The visual hovering and target following algorithm uses the implemented SURE-SLAM algorithm [10] for data processing. The SURE-SLAM algorithm is a vehicle-centric localization algorithm which is baed on computer-vision-based measurements using a stereo camera system observing the ground beneath the vehicle (ground relative navigation). This is accomplished by utilization of a SLAM (simultaneous localization and mapping) approach. Since a single camera cannot provide position information in 3d relative to a given target without additional information about the target (e.g. size, distance), a stereo camera system has to be used. A flow-chart for this implementation is shown in figure 1. The localization algorithm has three major parts: visual odometry, SLAM and the Kalman-filter (pose estimator). The visual odometry computes the motion between two camera image pairs (from the stereo camera system) by extracting and matching of SURF-features [11]. Its basic principle is shown in figure 2. The SLAM component keeps track of a global feature map and the vehicle's poses in form of a graph. It recognizes when the vehicle passes over a patch of ground it already passed before (loop-closing). As soon as such a loop-close occurs it is integrated into the graph as additional link, reducing the overall uncertainty (graph-based SLAM [12]). This way it can greatly reduce drift-induced deviation and increase long-term stability, similar to the effect of an LBL.

For the hovering algorithm the information of relative motion from the visual odometry portion is used with a keyframing method: instead of tracking the motion between each consecutive image a fixed keyframe image is used against which each consecutive image is tested. This results in a relative position between the current image and the keyframe image to be calculated, which is exactly the relevant information for hovering. The SLAM part of the SURE-SLAM algorithm is not used in this work.

By not being dependent on pre-defined targets, this method is very versatile and not limited to known terrain. In order to improve the station-keeping algorithm above, additionally specific objects can be segmented in the stereo camera images. This is useful when attempting to track a specific target (e.g. a buoy, markers). Apart from the object-specific segmentation the overall process remains the same. The main advantage of specific object tracking is its robustness to noise. While the generic feature-based approach can be used for specific objects as well, a dedicated detector/tracker will always out-perform a generic approach.

With the information about the relative position to the target (either a specific target or the keyframe) the vehicle controller attempts to reduce this distance to zero.

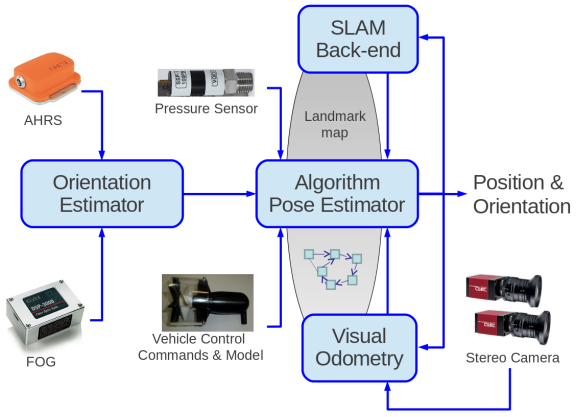

Fig. 1. Flow-chart of SURE-SLAM implementation on the AUV DAGON.

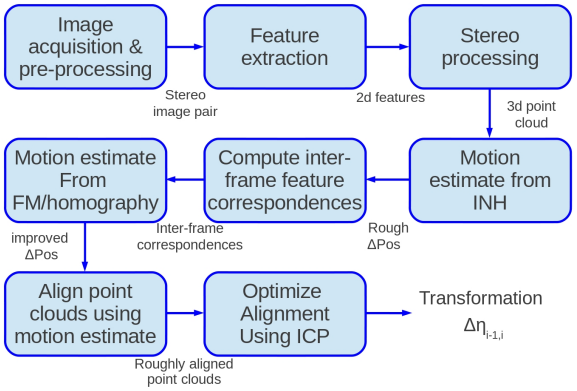

Fig. 2. The main steps in the visual odometry algorithm.

A. Performance Metrics

In order to assert the quality of hovering/tracking the following quantities will be used throughout the rest of this work:

The vehicle pose

$$\eta = [x, y, z, \phi, \theta, \psi] \tag{1}$$

in 6 DOFs, consisting of the vehicle position

$$\eta_1 = [x, y, z] \tag{2}$$

and its Euler orientation

$$\eta_2 = [\phi, \theta, \psi] \tag{3}$$

The position at a given point in time is denoted by the use of $\eta_1(i)$ where $i = 0$ is the initial position and $i = n$ is the final position of an experiment. The position difference between a frame and its predecessor is defined as

$$\eta_{1\Delta}(i) = \eta_1(i) - \eta_1(i-1) \tag{4}$$

The distance traveled as measured by the algorithm can then be defined as

$$|\eta| = \sum_{i=0}^{n} \eta_{1\Delta}(i) \tag{5}$$

The sparse deviation d_s is defined as

$$d_s = |\eta_1(0) - \eta_1(n)| \tag{6}$$

and denotes the distance between the position estimates of the start- and end of a test run for closed trajectories.

The sparse relative deviation $d_{r,s}$

$$d_{r,s} = \frac{d_s}{|\eta|} \tag{7}$$

is used for distance-normalized comparison.

II. EXPERIMENTS

In order to test the capabilities of the developed algorithms, experiments on a real vehicle (AUV Dagon [13]) were conducted in the test-tank of the underwater-testbed at the DFKI-RIC in Bremen. These tests on a live vehicle show the applicability of the methods used. Based on the experimental data, empirical performance characteristics are computed, giving the precision of station-keeping and target tracking using the visual hovering algorithm.

Since the test vehicle (see section II-A) is equipped with a DVL-based dead-reckoning navigation system the data recorded by this system can be used for comparison purposes. The differences between the visual tracking solution and the dead-reckoning solution can be considered the improvement over existing techniques when visual hovering/tracking is used. In order to verify the obtained results a technique called "sparse verification" is used: at the beginning of an experiment the vehicle position is manually enforced (i.e. it is pressed into a corner of the test tank). This initial position is regarded as zero position. At the end of an experiment this position again is manually enforced. An ideal algorithm would thus return to its origin position (with a slight tolerance due to measurement restriction when manually enforcing vehicle position). A realistic algorithm will have a non-zero deviation - comparing the deviations of different algorithms allows their objective comparison.

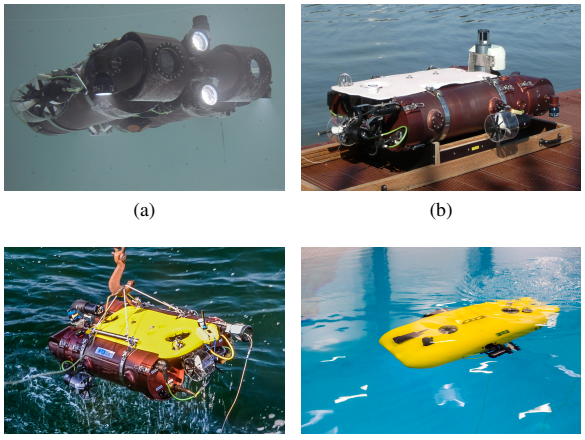

(a) (b) (c) (d)

Fig. 3. The AUV DAGON evolving: basic indoor testing (a); outdoor testing (b); open-water testing (2013); (c); current state (2014) with hydrodynamic hull (d).

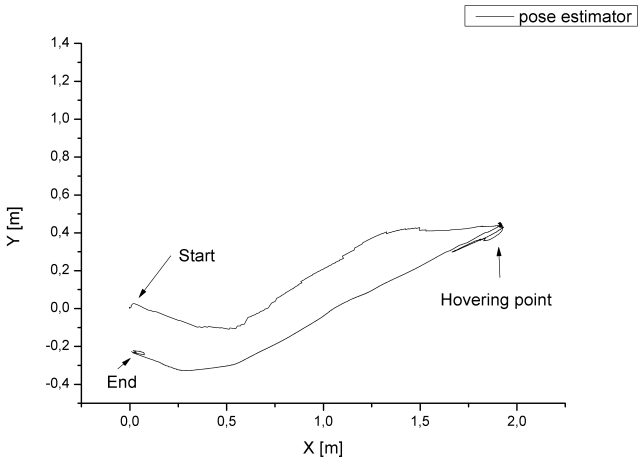

Fig. 4. Trajectory as estimated by the reference localization for the long-term hovering experiment. After starting in one corner of the glass tank the vehicle was hovering for 90 min in the center, and then returned to the initial position.

A. Descritpion of Vehicle

The vehicle which was used for all experiments withing this work is the AUV DAGON, which was developed as vehicle for development and evaluation of visual navigation algorithms. An overview of DAGON's instrumentation can be seen in table I. All of the required sensors could be integrated into the system. DAGON's evolution over the past years is shown in figure 3.

B. Hovering Indoors

In order to test the long-term stability of the hovering algorithm, an experiment was conducted in the glass tank. After initialization and manual enforcement of the starting position in one corner of the tank, the vehicle was moved to the center of the tank. There the station-keeping was activated and the vehicle kept hovering in the same place for 90 min. At the end, the vehicle was again returned to its starting point and the final position was manually corrected. The floor of the basin is covered with 16-32mm sized gravel. Both the dead-reckoning localization and SURE-SLAM localization were recorded. Figure 4 shows the estimated trajectory. The results were a deviation of $d_s = 0.2315\,\mathrm{m}$ after a traveled distance of $|\eta| = 11.3\,\mathrm{m}$, resulting in a relative deviation of $d_r = 2.05\,\%$ measured by the reference-localization. The orientation error was 2°. The SURE-SLAM measurement resulted in a $d_s = 0.0172\,\mathrm{m}$ after a traveled distance of $|\eta| = 5.2\,\mathrm{m}$, resulting in a relative deviation of $d_r = 0.332\,\%$. No orientation error was present in the SURE-SLAM measurement. The shorter $|\eta|$ measurement for SURE-SLAM stems from the fact that since during position-keeping keyframing was used, the maximum length of the graph is very low. For a completely dead-reckoning based approach there is no distinction between hovering and driving, resulting in an accumulation of small motion to a longer overall path.

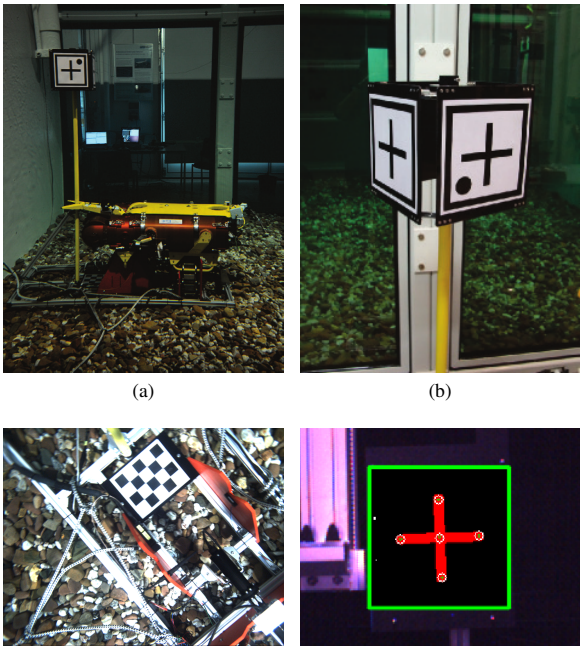

(a) (b) (c) (d)

Fig. 5. The markers used for target tracking. View of the complete docking-station with top and bottom markers (a); close-up of the top-marker (b); bottom marker as seen by the vehicle camera during docking (c); top marker as seen by the front camera during docking with processing overlay (d).

TABLE I
LIST OF SENSORS AND INSTRUMENTS OF THE AUV.

Instrument	Property	Rate	Precision	Range
XSens MTi AHRS	Attitude (R/P/Y)	120 Hz	0.5 ° (R/P) 1 ° (Y)	360 °
KVH DSP-3000 single axis FOG	Yaw rate	100 Hz	1-6 °/h^{-1}	±375 °s^{-1}
Desert Star SSP-1 pressure sensor	Depth	0.25 Hz to 16 Hz	0.1 % RMS	0 m to 344 m
Desert Star SAM-1 acoustic modem	Telemetry	23 bit s^{-1}	-	250 m to 1000 m
Desert Star VLT-3 LBL transponder	XYZ position	0.2 Hz to 2 Hz	±0.15 m	2000 m
Teledyne RDI Explorer DVL	Speed over ground	12 Hz	±0.007-0.03 m s^{-1}	0.3 m to 80 m
Micron DST scanning sonar	Distance	0.5 Hz[a]	-	2 m to 75 m
Micron USBL transponder	Range/Bearing[b]	0.1 Hz to 2 Hz	±0.2 m, ±3 °	150 m to 500 m
2 Bowtech LED3200	Illumination	22 kHz PWM	255 steps dimmable	-
2 AVT GE1900C GigE-cameras	Image	0-30 FPS	Full-HD (1920x1080)	-
1 AVT GC1380HC GigE-camera	Image	0-30 FPS	HD (1380x1024)	-

[a]For 360 ° scan
[b]Relative to receiver

C. Target Tracking

For target tracking a docking scenario was used for evaluation purposes. The docking station used was developed in order to prolong the vehicle DAGON's endurance. It is described in further detail in [14]. During the docking procedure target tracking is used at two of the docking stages: first the top marker is tracked during approach and later the bottom marker for precise adjustment of the final docking position. The docking-station and its markers are shown in figure 5. The top marker consists of four individual markers each consisting of a black cross on white background with a single black circle in one of the 4 quadrants encoding the 4 different marker sides. The bottom marker consists of a 4x3 chessboard as is used in camera calibration procedures (e.g. [15]). Both markers are detected by the respective modules of the OpenCV library [16].

For the target tracking a different evaluation method was used: since the docking-station offers a fixed relative position, the vehicle is regarded as non-moving. The movement measured by the tracking algorithm is thus directly the error of the algorithm. Since the dead-reckoning based solution is not feasible for tracking, only the measured error of the visual

tracking algorithm was recorded. For both the top and the bottom marker the measured error was below the reasonable sensing threshold. From the distance between the camera and the marker as well as the camera's resolution the maximally achievable accuracy can be calculated. For the experiments conducted this quantity was $5\,\mathrm{mm}$ ($60\circ$ opening angle of the camera, 640x480 pixels resolution, distance to target $50\,\mathrm{cm}$, target size $30\,\mathrm{cm}$).

III. Conclusion and Future Work

It could be shown that the visual hovering/tracking algorithm is capable of working on a live vehicle. The visual hovering component outperformed the dead-reckoning-based hovering by a significant margin, reducing the position error after 90 minutes of hovering from $0.2315\,\mathrm{m}$ to $0.0172\,\mathrm{m}$, a reduction of more than a magnitude. The target tracking algorithm was only tentatively evaluated. The achieved results for a static setup were within the expected bounds.

Future work will include outdoor tests of the algorithm. While the visual hovering capability has been used at numerous occasions while in the field, it was never possible to obtain sparse validation measurements in order to asses the method's objective performance. For the target tracking a dynamic scenario has to be selected which allows reasonable evaluation of the results. This can only be achieved when both the target and the vehicle's positions are known with high accuracy. This can be achieved for the target by having it moved by an external manipulator (e.g. an industrial gantry crane) with high precision position feedback. For the vehicle this is more complicated since in the hovering experiment it could be conclusively shown, that dead-reckoning-based localization is not up to the task.

For this work no new motion controller was implemented but the vehicle's position keeping controller (a two-stage PID-controller) was utilized. While sufficient for the experiments conducted in this work for highly dynamic scenarios this controller would need to be adapted.

Acknowledgment

The authors would like to thank all colleagues at DFKI GmbH, Robotics Innovation Center, Bremen for their support and feedback. The research leading to this results has received funding from the European Union Seventh Framework Program under the joint research activity of the EUROFLEETS2 project (grant No. 312762) and the German Federal Ministry of Economics and Technology (BMWi), project Europa-Explorer (grant No. 50NA1217).

References

[1] R. C. Arkin, *Behavior-based robotics*. MIT press, 1998.

[2] S. Thrun, "Probabilistic robotics," *Communications of the ACM*, vol. 45, no. 3, pp. 52–57, 2002.

[3] S. Negahdaripour, A. Shokrollahi, and C.-H. Yu, "Optical sensing for undersea robotic vehicles," *Robotics and autonomous systems*, vol. 7, no. 2, pp. 151–163, 1991.

[4] R. Marks, H. Wang, M. Lee, and S. Rock, "Automatic visual station keeping of an underwater robot," in *OCEANS '94. 'Oceans Engineering for Today's Technology and Tomorrow's Preservation.' Proceedings*, vol. 2, Sep 1994, pp. II/137–II/142 vol.2.

[5] K. Leabourne, S. Rock, S. Fleischer, and R. Burton, "Station keeping of an rov using vision technology," in *OCEANS '97. MTS/IEEE Conference Proceedings*, vol. 1, Oct 1997, pp. 634–640 vol.1.

[6] M. Caccia, "Vision-based rov horizontal motion control: Near-seafloor experimental results," *Control Engineering Practice*, vol. 15, no. 6, pp. 703–714, 2007.

[7] S. Desset, R. Damus, F. Hover, J. Morash, and V. Polidoro, "Closer to deep underwater science with odyssey iv class hovering autonomous underwater vehicle (hauv)," in *Oceans 2005 - Europe*, vol. 2, June 2005, pp. 758–762 Vol. 2.

[8] J. Vaganay, L. Gurfinkel, M. Elkins, D. Jankins, and K. Shurn, "Hovering autonomous underwater vehicle-system design improvements and performance evaluation results," in *Proceedings of the International Symposium on Unmanned Untethered Submersible Technology (UUST)*, 2009, pp. 1–14.

[9] S. Reed, J. Evans, B. Privat, and J. Wood, "Automated visual servoing for close inspection using low-cost, man-portable vehicles," in *Oceans - San Diego, 2013*, Sept 2013, pp. 1–6.

[10] M. Hildebrandt and F. Kirchner, "IMU-Aided Stereo Visual Odometry for Ground-Tracking AUV Applications," in *Proceedings of the IEEE OCEANS 10 Sydney*, 2010.

[11] H. Bay, A. Ess, T. Tuytelaars, and L. Van Gool, "Speeded-Up Robust Features (SURF)," *Computer Vision and Image Understanding*, vol. 110, no. 3, pp. 346–359, Jun. 2008. [Online]. Available: http://linkinghub.elsevier.com/retrieve/pii/S1077314207001555

[12] S. Fleischer, "Bounded-error vision-based navigation of autonomous underwater vehicles," Ph.D. dissertation, 2000. [Online]. Available: http://www.stanford.edu/group/arl/cgi-bin/drupal/sites/default/files/public/publications/Fleischer2000.pdf

[13] M. Hildebrandt and J. Hilljegerdes, "Design of a Versatile AUV for High Precision Visual Mapping and Algorithm Evaluation," in *Proceedings of the 2010 IEEE AUV Monterey*, Monterey, 2010.

[14] M. Wirtz, M. Hildebrandt, and C. Gaudig, "Design and test of a robust docking system for hovering AUVs," in *2012 Oceans*. Ieee, Oct. 2012, pp. 1–6. [Online]. Available: http://ieeexplore.ieee.org/lpdocs/epic03/wrapper.htm?arnumber=6404975

[15] Z. Zhang, "Flexible camera calibration by viewing a plane from unknown orientations," in *Computer Vision, 1999. The Proceedings of the Seventh IEEE International Conference on*, vol. 00, no. c, 1999, pp. 0–7. [Online]. Available: http://ieeexplore.ieee.org/xpls/abs_all.jsp?arnumber=791289

[16] Intel and WillowGarage, "OpenCV Library," 2013. [Online]. Available: http://sourceforge.net/projects/opencvlibrary/